Journal of Applied Polymer Science

Performance of Surface-Modified Poly(ether imide) Hollow-Fiber Membranes in a Membrane Gas—Liquid Contacting Process with Response Surface Methodology

G. Bakeri,[1] D. Rana,[3] A. F. Ismail,[2] T. Matsuura,[3] A. Ghaee[4]

[1]Faculty of Chemical Engineering, Babol Noshirvani University of Technology, Babol, Iran

[2]Advanced Membrane Technology Research Centre, Universiti Teknologi Malaysia, 81310 Skudai, Johor, Malaysia

[3]Industrial Membrane Research Laboratory, Department of Chemical and Biological Engineering, University of Ottawa, Ottawa, Ontario K1N 6N5, Canada

[4]Department of Life Science Engineering, Faculty of Interdisciplinary New Sciences and Technologies, University of Tehran, P. O. Box 14395-1561, Tehran, Iran

Correspondence to: A. F. Ismail (E-mail: afauzi@utm.my)

ABSTRACT: A surface-modifying macromolecule (SMM) was used to enhance the surface hydrophobicity of poly(ether imide) (PEI) hollow-fiber membranes. The membranes were used for a membrane contactor to absorb CO_2 with water. The effects of three hollow-fiber fabrication parameters, that is, the PEI concentration in the casting dope, the SMM concentration in the casting dope, and the air gap, on the liquid entry pressure of water (LEPw) and the absorption rate (AR) of CO_2 were investigated with response surface methodology. The model developed for LEPw satisfied the criterion for regression but had a low goodness of fit. The model predicted that LEPw would increase with PEI (weight percentage) but decrease with air gap. Furthermore, it showed a minimum value with a change in SMM (weight percentage). The model developed for the AR of CO_2 had meaningful statistical parameters and was accurate; this indicated that interactions existed between the fabrication parameters on the AR of CO_2. The performance of one of the fabricated membranes was compared with in-house and commercially made hydrophobic membranes in terms of the AR of CO_2 with distilled water as an absorbent on the lumen side and pure CO_2 on the shell side. The comparison showed a superior CO_2 flux in the surface-modified membrane; for example, at a liquid velocity of 0.4 m/s, the surface-modified membrane exhibited a 416% higher AR than the commercial membrane contactor (Celgard MiniModule 0.75X5) made of polypropylene. © 2012 Wiley Periodicals, Inc. J. Appl. Polym. Sci. 128: 1313–1325, 2013

KEYWORDS: applications; membranes; properties and characterization; separation techniques; structure–property relations

Received 6 May 2012; accepted 31 August 2012; published online 22 November 2012
DOI: 10.1002/app.38548

INTRODUCTION

The development of the chemical and petrochemical industries requires more efficient separation processes to reduce the cost and size of equipment. On the other hand, industrial development increasingly requires more water and produces more environmental pollution problems. More efficient technologies are called for to solve such problems. The use of clean and renewable energies (e.g., solar and wind energies) can decrease the emission of greenhouse gases into the environment, but those energies are generally more expensive than petroleum-based energies, and most countries cannot support these expenses to develop their use.

Furthermore, the increase of the world's population has intensified the difficulties in potable-water acquisition and wastewater treatment. The production of potable water from resources such as seawater is considered one of the methods needed to alleviate this serious burden. Nowadays, reverse osmosis (RO) is regarded as the most effective membrane process, but RO is generally expensive and faces its own problems, such as fouling and a low flux.

Membrane contactors are another membrane technology that can be used in various processes, such as gas absorption, membrane distillation water and wastewater purification etc. As the membrane does not contribute any significant resistance to the mass transfer between two streams, the flux through the membrane is usually much higher compared to the membranes in other membrane processes, such as gas separation and RO. It was also reported that the mass transfer per unit volume of a

membrane contactor is 2.7 times more than that in a packed column, a conventional piece of separation equipment.[1] It was also reported that membrane distillation is a strong competitor for RO for desalination because of its higher flux.[2]

To further reduce the membrane mass-transfer resistance, a membrane design based on a rational basis is desirable. Because the mass flux depends on the membrane properties, such as the surface porosity, overall porosity, and membrane tortuosity, the properties and structure of membrane should be properly adjusted. Furthermore, as the membrane pores are supposed to be gas-filled, the wettability of the membrane should be kept as low as possible; this also requires the proper adjustment of the pore size, surface roughness, chemical resistance to solvents, and hydrophobicity of membrane.[3] The wettability further depends on the operating conditions and the surface tension of the liquid. It was shown in our earlier work that the effect of the pore size on the wettability of a membrane was stronger than that of the hydrophobicity of the membrane,[4] and the polymeric material used for membrane preparation did not need to be too hydrophobic when the membrane pore size was sufficiently small. Nevertheless, the enhancement of the membrane surface hydrophobicity has been attempted by many researchers with methods such as low-temperature plasma treatment,[5,6] redox-initiated graft polymerization,[7] ion-beam irradiation,[8] photochemical grafting,[9,10] and UV-assisted grafting.[11]

One attractive method for changing the hydrophobicity of membranes is the blending of surface-modifying macromolecules (SMMs) in the casting dope. A hydrophobic SMM is a macromolecule with an amphipathic structure in which its main chain consists of a polyurea or polyurethane prepolymer (the hydrophilic part) and is end-capped with two low-polarity fluorine-based polymer (oligomer) chains (the hydrophobic part). When an SMM is blended in a host polymer solution, it tends to migrate to the polymer solution–air interface during the membrane fabrication process. Thus, the surface properties of the membrane are altered. The amount of SMMs that migrates to the membrane–air interface depends on parameters such as the molecular structure and molecular weight of the SMMs and the membrane fabrication conditions, for example, the temperature of the casting dope, the concentration of the host polymer, and the presence of SMMs and other additives in the casting dope. During migration, both ends of the SMM can further orient themselves vertically to the membrane–air interface; this increases the concentration of fluorine at the membrane surface.[12]

Many studies have been done on membrane surface modification with SMMs and the application of surface-modified membranes in various processes. However, most of them have been devoted to flat-sheet membranes, with a few exceptions devoted to hollow-fiber membranes.[12,13] Khayet et al.[14] used hydrophobic SMMs to alter the surface hydrophobicity of a poly(ether imide) (PEI) flat-sheet membrane to prepare a composite hydrophilic/hydrophobic membrane and applied the membrane in a direct-contact membrane distillation process. Pham et al.[15] applied hydrophobic SMMs to alter the surface properties of PEI flat-sheet membranes and intended to use them in pervaporation processes. Qtaishat et al.[16] used hydrophobic SMMs to change the hydrophobicity of PEI flat-sheet membranes, and their performance in a direct-contact membrane distillation process was investigated. Suk et al.[17] blended SMMs into a polyethersulfone (PES) casting solution and fabricated flat-sheet membranes. They also found that the fabricated membranes had the potential to be used in membrane distillation processes.

To the best of our knowledge, SMM-modified hollow-fiber membranes have been used for membrane contactors in only one study[18] for the removal of CO_2. On the other hand, in our earlier study,[19] the effects of the membrane fabrication parameters on the morphological properties of SMM-surface-modified membranes were investigated with response surface methodology (RSM). In particular, statistical methods were used to investigate the effects of the following three membrane fabrication parameters:

1. PEI concentration in the spinning dope.
2. SMM concentration in the spinning dope.
3. Air gap.

In a continuation of our earlier study,[19] the objective of this study was to investigate the effects of these three membrane fabrication parameters on the performance, including the liquid entry pressure of water (LEPw) and absorption rate (AR) of CO_2, of SMM-surface-modified PEI hollow-fiber membranes in membrane contactor applications. Again, RSM was used to analyze the experimental data. In RSM, all of the factors were changed at different levels simultaneously, and then, the best model was obtained with regression methods and optimization techniques.

THEORY

It is well known that application of statistical methods such as design of experiments makes the investigation of the effects of different factors on the process easier and enables us to survey a wider range of factor variation with a limited number of experiments.

In this study, central composite design in RSM was used to investigate the effects on the LEPw and CO_2 AR of the SMM-surface-modified membranes of the three fabrication parameters:

1. PEI concentration (weight percentage) in the spinning dope.
2. SMM concentration (weight percentage) in the spinning dope.
3. Air gap (centimeters).

In RSM, a model with the form of eq. (1) is fitted to the experimental data, and by optimization methods, the best coefficients for the model are calculated:

$$Y = a_0 + \sum_{i=1}^{f} a_i x_i + \sum_{i=1}^{f} a_{ii} x_i^2 + \sum_{i<j}^{f} a_{ij} x_i x_j + \zeta \qquad (1)$$

where f is the number of factors, x_i is a linear term, x_i^2 is a quadratic term, $x_i x_j$ is an interaction term, Y is the response (experimental data), ζ is the difference between the experimental data and the results predicted by the model, and a_i, a_{ii}, and a_{ij} are the coefficients of the model.

The methodology was described elsewhere in detail.[19] Briefly, the membranes were fabricated under a designed protocol, and the LEPw and CO_2 AR were measured. Minitab software (release 15, World Headquarters, PA USA) was used to analyze the results. The terms in the obtained model with a p value greater than 0.05 are deleted from the model if, after deletion of the term, the adjusted R^2 of the model increases. In other words, the term with the highest p value is deleted first followed by the step-by-step deletion of other terms with p values greater than 0.05. In some cases, after the deletion of a term with a p value greater than 0.05, the adjusted R^2 will decrease; this shows that this term has a little influence on the response and cannot be deleted. The adjusted R^2 shows a maximum value as these terms are deleted, and at the maximum value of the adjusted R^2, the truncation of terms of the model will be finished.

The final model should be verified in terms of regression and goodness of fit. The p value of regression should be less than 0.05,[20] whereas the p value for lack of fit should be greater than 0.05. The F-value for the model can be calculated using. $F\text{-}value_{regression} = MS\ for\ regression/MS\ for\ residual\ error$ which MS is mean of squares. The F-value for lack-of-fit can be calculated using. $F\text{-}value_{lack\text{-}of\text{-}fit} = MS\ for\ lack\text{-}of\text{-}fit/MS\ for\ pure\ error$ The F value can also be used to verify the model, where the F value for regression should be greater than the tabulated F value for the 95% confidence limit $[F_{0.05}^{tabulated}(f_1,f_2)]$, where f_1 is the degree of freedom for regression and f_2 is the degree of freedom for residual error. The F value for lack of fit should be less than the tabulated F value for the 95% confidence limit $[F_{0.05}^{tabulated}(f_3,f_4)]$, where f_3 is the degree of freedom for lack of fit and f_4 is the degree of freedom for pure error. Furthermore, R^2 and the adjusted R^2 of the model should be high.

The investigated factors and their levels are shown in Table I, where the axial spacing (α) value is 1.682.

EXPERIMENTAL

Materials

PEI (Ultem), used as the base polymer, was supplied from General Electric Company, United States *N*-Methyl-2-pyrrolidone (NMP; CAS number 872-50-4), with a purity of 99.5 wt %, was used as the solvent, and ethanol (CAS number 64-17-5), with a purity of 96 wt %, was used for the solvent-exchange process; both were purchased from Merck Company, Germany and were used without any purification.

The details of SMM synthesis were given elsewhere.[21] Methylene bis(*p*-phenyl isocyanate) (diphenylmethane diisocyanate), α,ω-aminopropyl poly(dimethyl siloxane), and Zonyl BA-L low fraction [2-(perfluoroalkyl)ethanol] were used for the synthesis of the SMMs. Elemental analysis and gel permeation chromatography (GPC; Waters Associates, Headquarters: Waters Corporation USA, GPC chromatograph equipped with a Waters 410 refractive-index detector) were used for the characterization of the synthesized SMMs. The results, the atomic percentage of fluorine and silicone obtained from elemental analysis and the number-average molecular weight (M_n) and polydispersity index (PDI), both obtained from GPC, are presented in Table II.

Table II. SMM Characterization Results

F (wt %)	Si (wt %)	M_n (10^4 g/mol)	PDI
16.21	12.82	1.62	1.82

PDI = Weight-average molecular weight/M_n.

The structure of the SMMs, determined from the previous characterization results, is shown in Figure 1, where p is the number of CF_2 repeating units and is equal to 7.58, n is the number of α,ω-aminopropyl poly(dimethyl siloxane) repeating units and is equal to 9.81, and m is the number of urea repeating units and is equal to 13.10.

Dope Preparation

PEI was dried at 70°C overnight. A predetermined amount of PEI was dissolved in NMP at 60–70°C under gentle stirring to prepare a 20 wt % PEI solution. A 6 wt % SMM solution was prepared by the dissolution of SMMs in NMP at room temperature under gentle stirring.

PEI and SMM solutions were combined to prepare the spinning dopes of desired compositions. Then, the solution was left standing for degassing.

Preparation of the Hollow Fibers

A dry–wet spinning process was used for the fabrication of the hollow-fiber membranes. The fabrication process was described elsewhere in detail.[22] A tube-in-orifice spinneret was used for dope extrusion. N_2 gas pressure was used to deliver the dope solution to a gear pump, by which the dope solution was brought to the annulus of the spinneret at a constant flow rate. Distilled water was used as the bore fluid and was delivered to the inner tube of the spinneret by a peristaltic pump at a constant flow rate.

After leaving the spinneret, the nascent hollow fiber passed through the air gap before entering the coagulant (water) bath to complete the phase-inversion process. The hollow fibers were then collected by a take-up drum and kept immersed in water for several days before the solvent exchange was conducted by

Table I. Investigated Factors and Their Levels in the Experimental Design

	Level				
Factor	−1.682	−1	0	1	1.682
PEI (wt %) in the casting dope	14 (13.9955)[a]	14.2	14.5	14.8	15 (15.0045)
SMM (wt %) in the casting dope	0.002 (0.00206)	0.51	1.255	2	2.508 (2.50794)
Air gap (cm)	0.89 (0.887)	21	50.5	80	100.1 (100.113)

The values in parentheses represent the designed values for factors, which were not applied in the experimental runs.

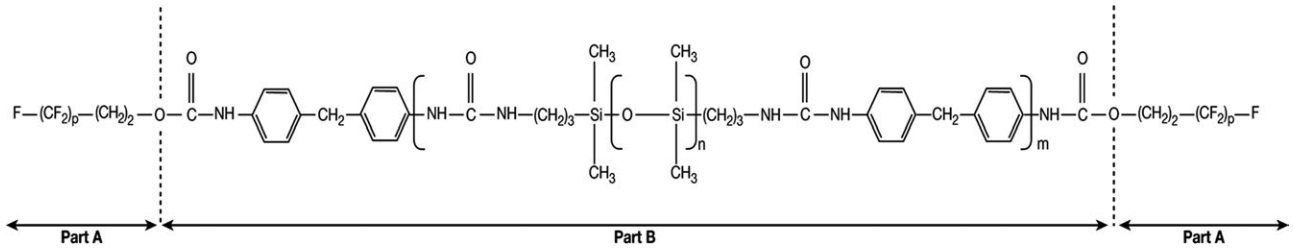

Figure 1. Structure of SMM.

the immersion of the hollow fibers in water/ethanol mixtures with progressively higher ethanol concentrations:

1. 1 h in a 33 wt % ethanol solution in water.
2. 1 h in a 66 wt % ethanol solution in water.
3. 2 h in pure ethanol.

We dried the hollow fibers further naturally by hanging them vertically for 1–2 days at ambient temperature. The spinning conditions are listed in Table III.

Measurement of the LEPw

The wettability of the membrane in contactor applications should be low because the penetration of liquid into the membrane pores drastically reduces the performance of the contactor. The LEPw is a criterion of the wettability of membrane and is defined as the minimum pressure needed to push water through the membrane pores. As the biggest pores wet first, this test depends on the maximum pore size of the membrane.

Two to three hollow fibers were glued with epoxy resin at one end, and the other end was potted to stainless steel tubing with a diameter of 1.4 cm. The latter end was cut with a sharp knife after the epoxy resin hardened to open the hollow fibers.[23] Water was sent with a peristaltic pump to the lumen side of the fibers, and the pressure of water was gradually increased with a step size of 0.5 bar. The water was kept at each pressure for about 30 min. The pressure at which the first droplet of water appeared on the outer surface of the membrane was reported as the LEPw.

Gas Absorption Test

A gas absorption test was used to evaluate the performance of the fabricated hollow-fiber membranes in contactor applications. Some hollow-fiber membranes were assembled in a contactor module with a diameter of 1.565 cm. Pure CO_2, with a gauge pressure of 1 bar, was sent to the shell side of the contactor with a volumetric flow rate of 1 L/min, whereas distilled water, with a gauge pressure of 1.5 bar, was used as the absorbent and was sent to the lumen side of the hollow fibers at a flow velocity of 0.1 m/s unless otherwise stated. The high gas velocity in the shell side of the contactor guaranteed low mass-transfer resistance on the shell side of the contactor.

Table III. Hollow-Fiber Spinning Conditions

Polymer concentration (wt %)	On the basis of the designed experiments shown in Table IV
SMM concentration (wt %)	On the basis of the designed experiments shown in Table IV
Air gap (cm)	On the basis of the designed experiments shown in Table IV
Bore fluid	Distilled water
External coagulant	Tap water
Bore fluid temperature (°C)	Room temperature
External coagulant temperature (°C)	Room temperature

The membrane contactor system is shown schematically in Figure 2. A diaphragm pump was used to supply distilled water at a constant pressure. The flow rate of water was controlled by a valve at the exit of the contactor module.

The flow rate of absorbent was changed, and the amount of absorbed CO_2 was measured by the titration of exit water with a 0.5*M* sodium hydroxide (NaOH) solution as the titrant and a phenolphthalein solution as the indicator. Then, the overall absorption flux of CO_2 was calculated with the flow rate of water and the concentration of CO_2 in water at the exit and was reported as moles of CO_2 per square meter per second.

RESULTS AND DISCUSSION

The designed experiments in their coded and uncoded forms are shown in Table IV. The response values, the LEPw and AR of CO_2, corresponding to each run are also shown in Table IV. Membranes M5 and M13 were wetted before the contactor test was carried out because of their low LEPws. The AR of CO_2 for these membranes was considered to be zero.

To compare the LEPw and AR of CO_2 between the membranes with and without SMMs, hollow fibers were spun under the same fabrication conditions but without SMMs. The fabrication conditions and the performance results are shown in Table V.

t-value: Test statistic for the t-test family, it measures the difference between an observed statistic and its hypothesized population parameter in units of standard error. A *t*-test compares this observed t-value to a critical value on the *t*-distribution with (n-1) degrees of freedom to determine whether the difference between the estimated and hypothesized values of the population parameter is statistically significant.

Analysis of Variance (ANOVA) for the LEPw

RSM in Minitab software (release 15) was used to find the best model for the LEPw. The estimated coefficients for the model in terms of coded factors and the *t* value and *p* value for each coefficient are shown in Table VI.

The significance of the terms in the model could be ranked with a student's *t* test, as the term with the lowest *p* value and the highest

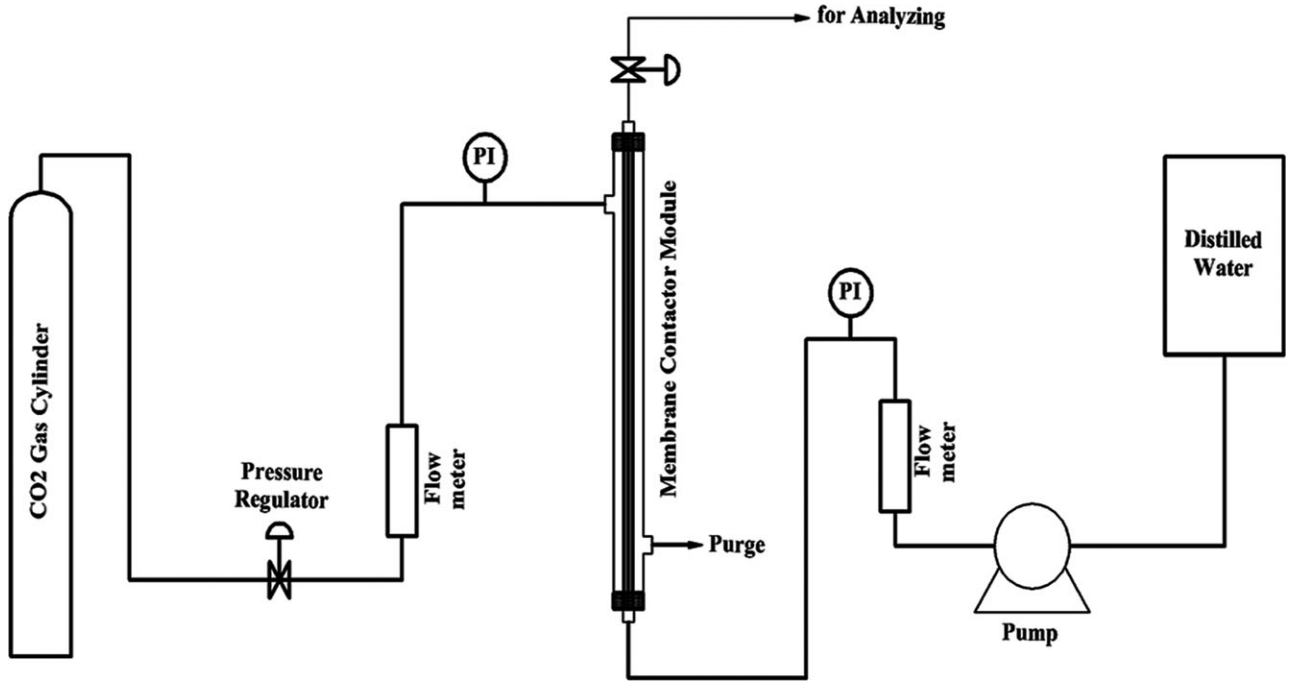

Figure 2. Schematic of the membrane contactor test system. PI, pressure indictor.

Table IV. Designed Experiments and Output Responses for the SMM-Surface-Modified PEI Membranes

		Fabrication parameter						Response	
		PEI in the dope solution (x_1)		SMM in the dope solution (x_2)		Air gap (x_3)			
Membrane number	Run type[a]	wt %	Level[b]	wt %	Level[b]	cm	Level[b]	LEPw (bar)	AR, liquid in lumen side, V_{liquid} = 0.1 m s^{-1} (mol m^{-2} s^{-1})
M1	A	15.0	α	1.255	0	50.5	0	0.5	1.20×10^{-3}
M2	A	14.0	$-\alpha$	1.255	0	50.5	0	0.5	1.18×10^{-3}
M3	A	14.5	0	2.508	α	50.5	0	2.5	1.19×10^{-3}
M4	A	14.5	0	0.002	$-\alpha$	50.5	0	2.5	1.25×10^{-3}
M5	A	14.5	0	1.255	0	100.1	α	0	0
M6	A	14.5	0	1.255	0	0.89	$-\alpha$	1.5	1.44×10^{-3}
M7	O	14.8	1	2.0	1	80.0	1	0.5	1.06×10^{-3}
M8	O	14.8	1	2.0	1	21.0	−1	3.5	1.19×10^{-3}
M9	O	14.8	1	0.51	−1	80.0	1	0.5	9.93×10^{-4}
M10	O	14.8	1	0.51	−1	21.0	−1	3.5	1.21×10^{-3}
M11	O	14.2	−1	2.0	1	80.0	1	0.5	8.40×10^{-4}
M12	O	14.2	−1	2.0	1	21.0	−1	2.5	1.64×10^{-3}
M13	O	14.2	−1	0.51	−1	80.0	1	0.5	0
M14	O	14.2	−1	0.51	−1	21.0	−1	2.5	1.27×10^{-3}
M15	C	14.5	0	1.255	0	50.5	0	0.5	1.12×10^{-3}
M16	C	14.5	0	1.255	0	50.5	0	0.5	1.29×10^{-3}
M17	C	14.5	0	1.255	0	50.5	0	0.5	1.17×10^{-3}
M18	C	14.5	0	1.255	0	50.5	0	0.7	8.90×10^{-4}
M19	C	14.5	0	1.255	0	50.5	0	0.7	1.12×10^{-3}
M20	C	14.5	0	1.255	0	50.5	0	0.5	1.20×10^{-3}

[a]C, center point; O, orthogonal design or cube point; A, star or axial point. [b]−1, low value; 0, center value; 1, high value; $\pm\alpha$, star or axial point value.

Table V. Characterization Test Results for the PEI Membranes without SMMs

	Fabrication parameter		Responses	
Membrane number	PEI in the dope solution (wt %)	Air gap (cm)	LEPw (bar)	AR, liquid in lumen side [V_{liquid} = 0.1 m/s (mol m^{-2} s^{-1})]
M21	14.0	50.5	2.5	1.02×10^{-3}
M22	14.2	21.0	3.5	1.08×10^{-3}
M23	14.2	80.0	1.5	NA
M24	14.5	0.89	2.0	1.71×10^{-3}
M25	14.5	50.5	2.5	1.05×10^{-3}
M26	14.5	100.1	2.5	7.95×10^{-4}
M27	14.8	21.0	3.0	9.58×10^{-4}
M28	14.8	80.0	2.0	8.16×10^{-4}
M29	15.0	50.5	2.5	1.21×10^{-3}

NA, not available.

t value was the most significant term in the model. The significant terms in the model for the LEPw were ranked as follows:

$$x_2^2 > x_3 > x_1x_3 > x_3^2 > x_1 > x_2$$

ANOVA was used to qualify the regression equation, and the ANOVA table at the 95% confidence limit for the model developed for the LEPw is presented in Table VII.

The adequacy of the model was analyzed by the data presented in Table VII. The *F* value for the model was 14.49, which was greater than $F_{0.05}(f_1,f_2)$ [$F_{0.05}(f_1,f_2) = F_{0.05}(6,13) = 2.9153$], but the *F* value for lack of fit was 36.31, which was not smaller than $F_{0.05}(f_3,f_4)$ [$F_{0.05}(f_3,f_4) = F_{0.05}(8,5) = 4.8183$]. In other words, the model satisfied the criterion for regression, but its goodness of fit was not suitable. This conclusion was further confirmed by the *p* values for regression and lack of fit as the *p* value for regression was smaller than 0.05, but the *p* value for lack of fit was not greater than 0.05. R^2 for the model was 86.99%; this indicated that 86.99% of the variations in the experimental data could be explained by the model. In addition, the adjusted R^2 was 80.99%, which was a high value for adjusted R^2.[24]

The predicted values for LEPw by the model were compared with the experimental results in Figure 3; this showed that the predicted values had a lack of fit with the experimental results that could have been due to the large step size of 0.5 bar, which caused large experimental errors. A smaller step size for the pressure increase should have been chosen.

The comparison of the results presented in Tables IV and V for the LEPw values of the membranes with and without SMMs showed that membranes with SMMs had lower LEPws; this was related to their higher pore size, even though SMM-surface-modified membranes had a higher contact angle with water.[19]

Effect of the Membrane Fabrication Parameters on LEPw

The surface plots of the LEPw versus two fabrication parameters with the third parameter held constant at its central value are shown in Figure 4(a–c).

Table VI. Estimated Regression Coefficients (Coded Factors); Response: LEPw

Term	Coefficient	SE coefficient	*t*	*p*
Constant	0.61181	0.1705	3.589	0.003
x_1: PEI (wt %)	0.24631	0.2241	1.099	0.292
x_2: SMMs (wt %)	0.00000	0.2241	0.000	1.000
x_3: Air gap (cm)	−1.54210	0.2241	−6.882	0.000
x_2^2: SMMs (wt %) × SMMs (wt %)	2.18647	0.3650	5.990	0.000
x_3^2: Air gap (cm) × Air gap (cm)	0.43644	0.3650	1.196	0.253
x_1x_3: PEI (wt %) × Air gap (cm)	−0.70709	0.4923	−1.436	0.175

Standard error for the estimated coefficient (SE Coefficient). A standard error for an estimated coefficient measures the precision of the estimate. The smaller the standard error, the more precise is the estimate.

Table VII. ANOVA Table for the Model; Response: LEPws of the SMM-Modified Membranes

Source	DF	Seq. SS	Adjusted SS	Adjusted MS	*F*	$F^{tabulated}$	*p*
Regression	6	21.0780	21.0780	3.51300	14.49	2.9153	0.000
Residual error	13	3.1515	3.1515	0.24242			
Lack of fit	8	3.0981	3.0981	0.38727	36.31	4.8183	0.001
Pure error	5	0.0533	0.0533	0.01067			
Total	19	24.2295					

R^2 = 86.99%, adjusted R^2 = 80.99%. DF, degrees of freedom; SS, sum of squares; MS, mean square.
Sequential sums of squares (Seq. SS). The Seq. SS for a predictor measures the increase in the SS Regression when the predictor is added to a model involving only the predictors listed before it.

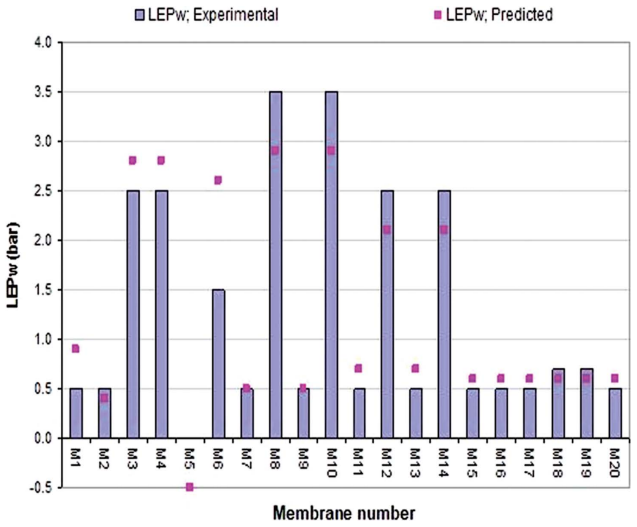

Figure 3. Comparison of the experimental results and the values predicted by a model for LEPw for membranes with SMM. [Color figure can be viewed in the online issue, which is available at wileyonlinelibrary.com.]

As shown in Figure 4(a), the LEPw had an increasing trend versus PEI (weight percentage); this means that the maximum pore size of the membrane decreased as the weight percentage of PEI increased. On the other hand, as shown in Figure 4(a,b), the LEPw showed a minimum value as the weight percentage of SMMs increased. Even though it was reported that the LEPw did not correlate to the mean pore size of a membrane,[4] it was interesting to note that the trend in the LEPw versus weight percentage of SMMs was in accordance with the trend observed in the mean pore size versus the weight percentage of SMMs, as reported elsewhere.[19] In other words, as the weight percentage of SMMs increased, the pore size of the membrane increased; this led to a decrease in the LEPw. However, when the SMM weight percentage was beyond a specific value, the pore size of the membrane decreased, and also, the hydrophobicity of the membrane increased because of the higher concentration of SMMs. This led to an increase in the LEPw. Furthermore, the effect of SMMs on the pore blocking should have been taken into consideration, especially at higher concentrations of SMM.

As shown in Figure 4(b,c), the LEPw showed a decreasing trend versus the air gap. Because the LEPw depended on the maximum pore size of the membrane, the maximum pore size of the membrane increased as the air gap increased. The same result was reported elsewhere[13] as the tail of the pore size distribution curve extended to a bigger pore size as the air gap increased. This phenomenon could have been related to the elongation of fibers at the higher air gap, which eliminated the small pores and increased the size of bigger pores. This trend was confirmed by the scanning electron microscopy (SEM) images taken of the outer surface of membranes M6, M16, and M5 with a magnification of 50,000 (Figure 5); these showed that the maximum pore size of the membrane increased as the air gap increased.

ANOVA for the AR, Liquid in the Lumen Side

RSM in Minitab software (release 15) was used to find the best model for the AR, liquid in the lumen. The estimated coefficients for the model in terms of coded factors and the t value and p value for each coefficient are shown in Table VIII.

The student's t test was used to determine the significance of the terms in the model. The significant terms in the model for the AR, liquid in the lumen could be ranked as follows:

$$x_3 > x_1x_3 > x_3^2 > x_1x_2 > x_2 > x_1 > x_2x_3 > x_2^2 > x_1^2$$

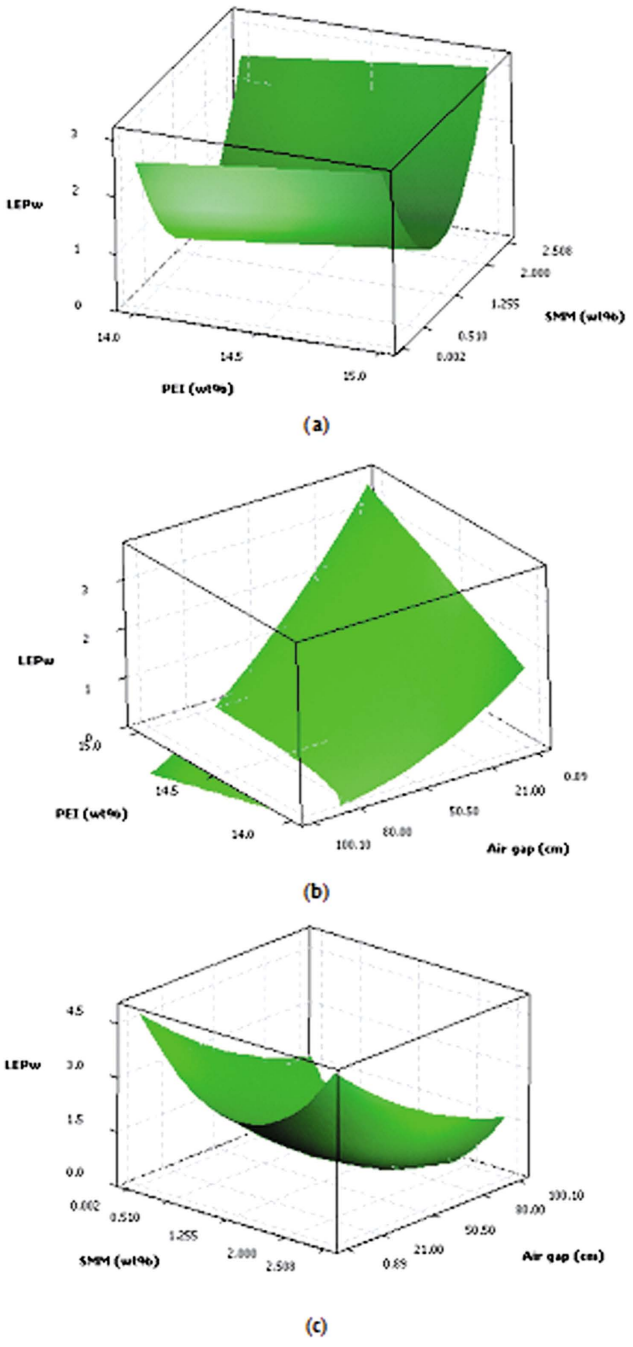

Figure 4. Surface plots for LEPw: (a) PEI (wt %) and SMM (wt %); air gap value = 50.5 cm, (b) PEI (wt %) and air gap (cm); SMM = 1.255 wt %, and (c) SMM (wt %) and air gap (cm); PEI value = 14.5 wt %. [Color figure can be viewed in the online issue, which is available at wileyonlinelibrary.com.]

Applied Polymer SCIENCE

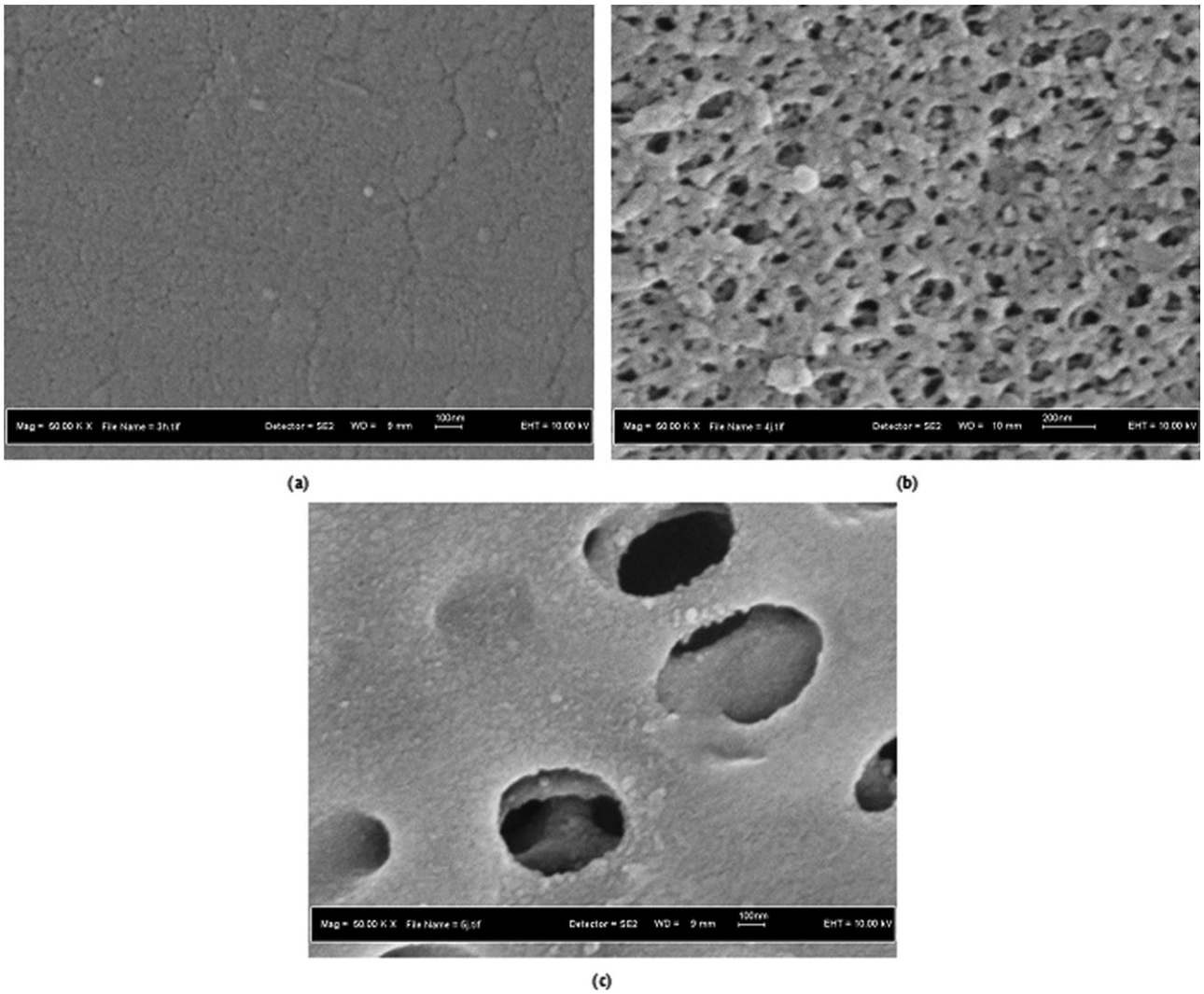

Figure 5. SEM micrographs of the membranes' outer surfaces: (a) M6 (air gap = 0.89 cm), (b) M16 (air gap = 50.5 cm), and (c) M5 (air gap = 100.1 cm). The PEI concentration and SMM concentration were maintained at 14.5 and 1.255 wt %, respectively.

ANOVA is a useful tool for qualifying the regression equation, and the ANOVA table at the 95% confidence limit for the model developed for the AR, liquid in the lumen is presented in Table IX.

The adequacy of the model was analyzed. As shown in Table IX, the F value for the model was 10.83, which is greater than $F_{0.05}(f_1,f_2)$ [$F_{0.05}(f_1,f_2) = F_{0.05}(9,10) = 3.0204$], and the F value for lack of fit was 2.21, which was smaller than $F_{0.05}(f_3,f_4)$

Table VIII. Estimated Regression Coefficients (Coded Factors); Response: AR, Liquid in the Lumen

Term	Coefficient	SE Coefficient	t	p
Constant	1.13×10^{-3}	6.90×10^{-5}	16.400	0.000
x_1: PEI (wt %)	9.20×10^{-5}	7.70×10^{-5}	1.193	0.261
x_2: SMM (wt %)	1.43×10^{-4}	7.70×10^{-5}	1.864	0.092
x_3: Air gap (cm)	-5.95×10^{-4}	7.70×10^{-5}	−7.737	0.000
x_1^2: PEI (wt %) × PEI (wt %)	5.40×10^{-5}	1.26×10^{-4}	0.429	0.677
x_2^2: SMM (wt %) × SMM (wt %)	8.30×10^{-5}	1.26×10^{-4}	0.659	0.525
x_3^2: Air gap (cm) × Air gap (cm)	-4.19×10^{-4}	1.26×10^{-4}	−3.326	0.008
x_1x_2: PEI (wt %) × SMM (wt %)	-4.11×10^{-4}	1.69×10^{-4}	−2.429	0.036
x_1x_3: PEI (wt %) × Air gap (cm)	6.09×10^{-4}	1.69×10^{-4}	3.599	0.005
x_2x_3: SMM (wt %) × Air gap (cm)	1.96×10^{-4}	1.69×10^{-4}	1.162	0.272

Table IX. ANOVA Table for the Model; Response: AR, Liquid in the Lumen of the SMM-Modified Membranes

Source	DF	Seq. SS	Adjusted SS	Adjusted MS	*F*	$F^{tabulated}$	*p*
Regression	9	3.00×10^{-6}	3.00×10^{-6}	0	10.83	3.0204	0.000
Residual error	10	0	0	0			
Lack of fit	5	0	0	0	2.21	5.0503	0.203
Pure error	5	0	0	0			
Total	19	3.00×10^{-6}					

R^2 = 90.69%; adjusted R^2 = 82.32%.DF, degrees of freedom; SS, sum of squares; MS, mean square.

$[F_{0.05}(f_3,f_4) = F_{0.05}(5,5) = 5.0503]$. Also, the *p* value for the model was smaller than 0.05, and the *p* value for the lack of fit was greater than 0.05. R^2 for the model was 90.69%; this means that only 9.31% of the variations in the experimental data could not be explained by the model. Furthermore, the adjusted R^2 was 82.32%, which is a high value for adjusted R^2. So, the model developed for the AR, liquid in the lumen was adequate.

The predicted values for the AR, liquid in the lumen by the model are compared with experimental results in Figure 6, which shows that the predicted values had good fits with the experimental results.

A comparison of the AR of CO_2 for the PEI hollow-fiber membranes with and without SMM (as shown in Tables IV and V) indicated that the AR of CO_2 for the surface-modified membranes was generally higher. The ARs of CO_2 for membranes M7 and M28 and membranes M17 and M25 over a wide range of liquid velocity (V_{liquid}) are shown in Figures 7 and 8, respectively. The figures indicate that as V_{liquid} increased, the difference in the ARs between these two types of membranes increased. At a V_{liquid} as low as 0.1 m/s, the liquid-side mass-transfer resistance seemed predominant, and the difference between the different types of membranes was not quite observable. However, the choice of 0.1 m/s could be justified by the fact that at a flow velocity as high as 1 m/s, the pressure drop from the inlet to the outlet of some hollow fibers became too high because of their small inner diameters, and inlet pressures higher than the LEPw were required. Moreover, RSM analysis conducted at 0.3 m/s resulted in almost the same conclusions as the analysis at 0.1 m/s.

The higher ARs of CO_2 for the PEI membranes with SMMs (M7 and M17) compared to those of the PEI membranes without SMMs (M28 and M25) were due to the change in membrane properties.

The data shown in Figures 7 and 8 indicate that the CO_2 ARs of the SMM-modified membranes (M7 and M17) were higher than those of the membranes without SMM modification (M28 and M25) when the liquid boundary layer was removed. In general, SMM-modified membranes have features of a lower membrane bulk porosity and lower LEPw but have a higher membrane surface porosity, higher mean pore size, and higher contact angle of water. The higher membrane surface porosity and pore size enhanced the CO_2 AR. On the other hand, the higher mean pore size was compensated by the larger contact

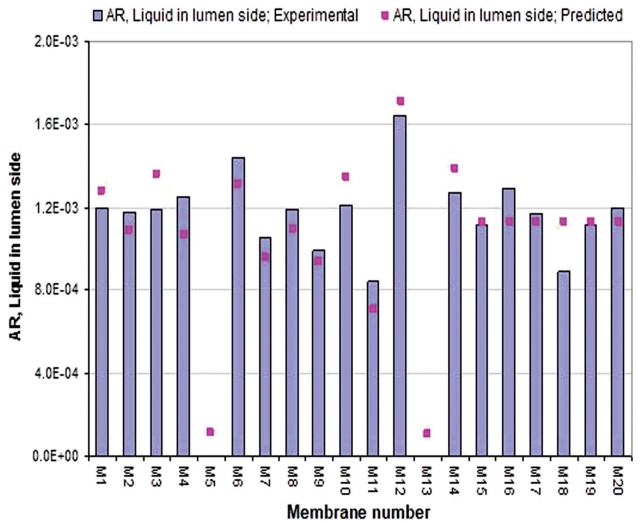

Figure 6. Comparison of the experimental results and the values predicted by the model for the AR, liquid in the lumen for membranes with SMM. [Color figure can be viewed in the online issue, which is available at wileyonlinelibrary.com.]

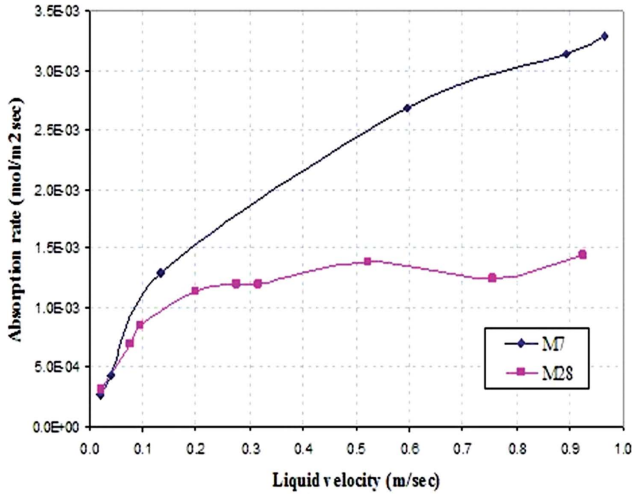

Figure 7. Variation of the AR of CO_2 for the M7 (with SMM) and M28 (without SMM) membranes versus V_{liquid} with pure CO_2 in the shell side and distilled water in the lumen side. [Color figure can be viewed in the online issue, which is available at wileyonlinelibrary.com.]

Applied Polymer SCIENCE

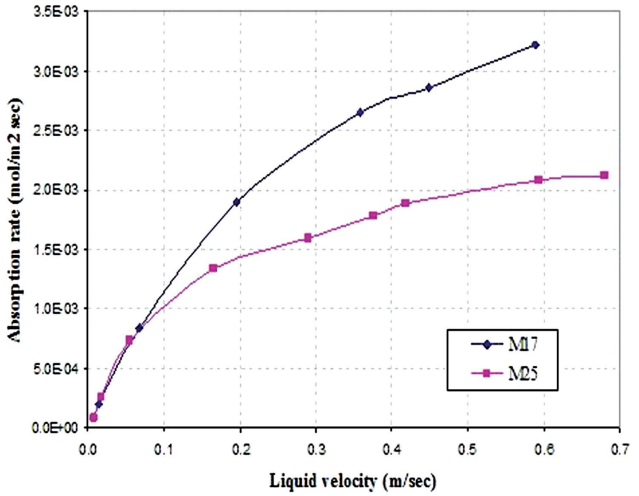

Figure 8. Variation of the AR of CO_2 for the M17 (with SMM) and M25 (without SMM) membranes versus V_{liquid} with pure CO_2 in the shell side and distilled water in the lumen side. [Color figure can be viewed in the online issue, which is available at wileyonlinelibrary.com.]

angle and did not necessarily increase the wettability. Thus, the SMM surface modification produced more favorable results.

Effect of the Membrane Fabrication Parameters on the AR, Liquid in the Lumen

The surface plots of the AR, liquid in the lumen versus two fabrication parameters with the third parameter held constant at its central value are shown in Figure 9(a–c).

As shown in Figure 9(a–c), the effects of the fabrication parameters on the AR, liquid in the lumen were interrelated. For example, Figure 9(b) shows that at a low air gap, the AR, liquid in the lumen decreased as the PEI concentration increased, whereas at a high air gap, it increased as the PEI concentration increased. This interaction was ascribed to the fact that the absorption flux in a membrane contactor is a complex function of various parameters, including the structure (e.g., membrane porosity and tortuosity) and morphology of the membrane and the operating conditions of the absorption process (e.g., temperature, pressure, type and flow rates of streams).[25] The *surface porosity*, which is defined as the ratio of the area of pores to the total area of the membrane, determines the effective part of membrane area for mass diffusion through a membrane. Therefore, the higher the surface porosity was, the higher will the AR became. Also, the larger the pore size was, the higher the AR became. However, the larger pore size enhanced the wettability of the membrane, even when the membrane was hydrophobic. Furthermore, pore condensation is another factor that reduces the performance of a membrane contactor regardless of the membrane wettability.

For a given porosity, the location of the pores is another factor that governs membrane performance. It was reported that the distance between pores also affects the performance of a contactor.[26] When the ratio of the distance between adjacent pores to the liquid-side boundary layer thickness is small, all of the membrane area is effective in mass transfer between gas and liquid streams. As it is known, the liquid-side boundary layer thickness depends on V_{liquid} and the type of absorption (physical or chemical) process. Furthermore, the partial wetting of membrane pores during the absorption process should be considered, as reported by Mavroudi et al.,[27] because this phenomenon reduces the AR at the beginning of the absorption process. Briefly, the interpretation of the adsorption rate data is more difficult than is usually thought.

Figure 9(a) shows that at low SMM concentrations, the AR, liquid in the lumen increased as the PEI concentration increased, whereas at high SMM concentrations, the trend was reversed. This phenomenon could be related to the variation in the membrane pore size and porosity. At low SMM concentrations, an increasing PEI concentration reduced the pore size of the

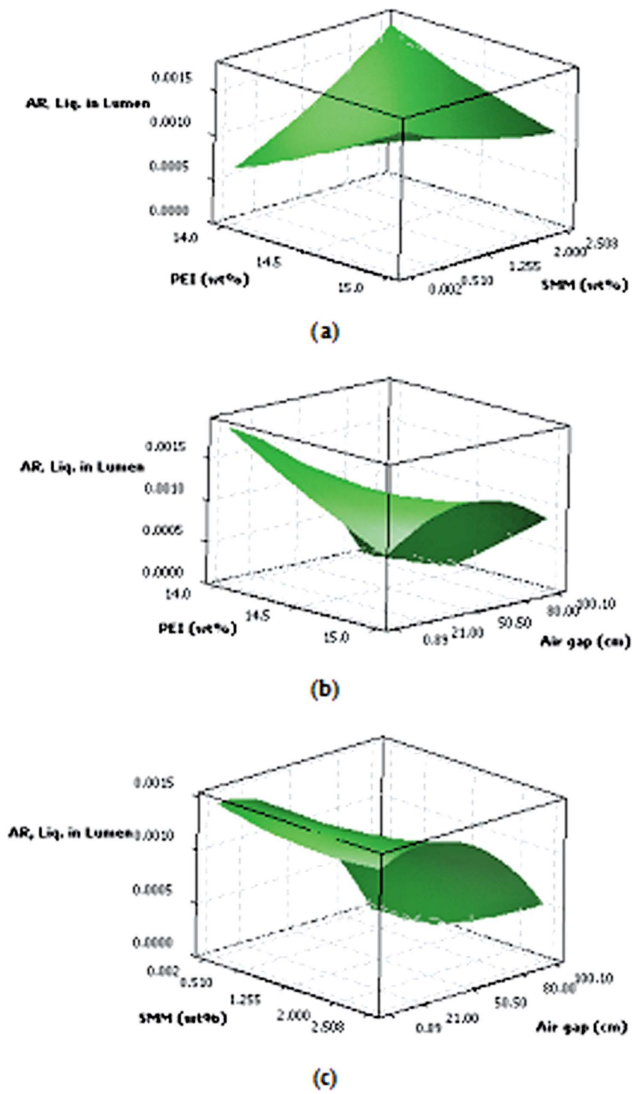

Figure 9. Surface plots for the AR, liquid in the lumen: (a) PEI (wt %) and SMM (wt %); air gap value = 50.5 cm, (b) PEI (wt %) and air gap (cm); SMM value = 1.255 wt %, and (c) SMM (wt %) and air gap (cm); PEI value = 14.5 wt %. [Color figure can be viewed in the online issue, which is available at wileyonlinelibrary.com.]

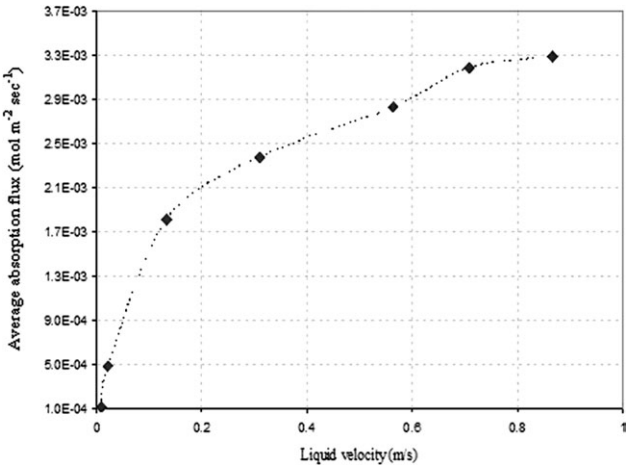

Figure 10. Variation of the average absorption flux of CO_2 for the M12 membrane with V_{liquid} with distilled water in the lumen side and pure CO_2 in shell side.

membrane and, consequently, the pore wetting, whereas at high SMM concentrations, the SMMs migrated to the surface and partially blocked the pores; this reduced the surface porosity. An increase in the PEI concentration further reduced the pore size and led to a decrease in the AR. This explanation could also be used for the effect of the SMM concentration on the AR; that is, at high PEI concentrations, an increase in the SMM concentration reduced the membrane pore size and increased the mass-transfer resistance of the membrane [see Figure 9(a)].

The effect of the air gap on the AR was more complicated. As shown in Figure 9(b), the AR, liquid in the lumen decreased with the air gap at low PEI concentrations, whereas at high PEI concentrations, the AR, liquid in the lumen showed a maximum value. A similar maximum was also found, as shown in Figure 9(c), for a given SMM concentration. The membrane porosity and LEPw of membrane decreased as the air gap increased; this had a negative effect on the AR. On the other hand, the contact angle of water with the surface of the membrane had a maximum value versus the air gap, where the maximum value increased with increasing concentration of PEI or SMM.[19] As the contact angle is an indicator of the wettability of a membrane, a higher contact angle means a lower mass-transfer resistance due to the wetting of membrane. So, the presence of the maximum point in the AR, liquid in the lumen versus the air gap could have been related to the reduction in the membrane wettability.

To evaluate the performance of the surface-modified membranes in contactor applications, the AR of CO_2 for membrane M12 was measured over a range of V_{liquid} values, as shown in Figure 10, and was compared with the AR of CO_2 for other in-house and commercially made membranes, as presented in Table X. The M12 membrane was chosen for this purpose because it showed the highest CO_2 flux among all of the SMM-modified membranes. As Figure 10 shows, the absorption flux increased strongly with increased V_{liquid}.

Atchariyawut et al.[28] blended different types of nonsolvents with a polyvinylidene fluoride (PVDF) solution and fabricated

Table X. Comparison of the ARs of CO_2 for the M12 Membrane with Membranes Made In-House and Commercially

Membrane type	Mean pore size (nm)	Membrane porosity (%)	ID (mm)	OD (mm)	LEPw (bar)	Effective fiber length (cm)	Number of fibers	Absorption flux (mol m^{-2} s^{-1})	Fluid in lumen side	Manufacturer	Reference
PVDF	20[a]	76.02	0.514	0.828	NA	25	8–10	1.2×10^{-3}[b]	Pure CO_2	Made in-house	28
PP[c]	40	40	0.22	0.3	NA	11.3	1100	0.5×10^{-3}[b]	Water	Celgard, Inc.	29
Porous PVDF	200	75	0.65	1	NA	27	35	3.5×10^{-3}[d]	2M NaOH	Memcor Australia	30
Porous PVDF	200	75	0.65	1	NA	27	35	1.1×10^{-3}[d]	Water	Memcor Australia	30
PP	640[e]	79[f]	0.6	1	NA	27	1	2.53×10^{-3}[g]	Water	Membrana Germany PP Q3/2	31

NA, not available. [a]Determined by the solute-rejection method. [b]Achieved at $V_{liquid} = 0.4$ m/s. [c]Celgard MiniModule 0.75X5 commercial contactor. [d]Achieved at $V_{liquid} = 1$ m/s. [e]Maximum pore size. [f]From Sep. Purif. Technol. 2002, 27, 231. [g]Achieved at $V_{liquid} = 0.5$ m/s^{-1}, PP,polypropylene.

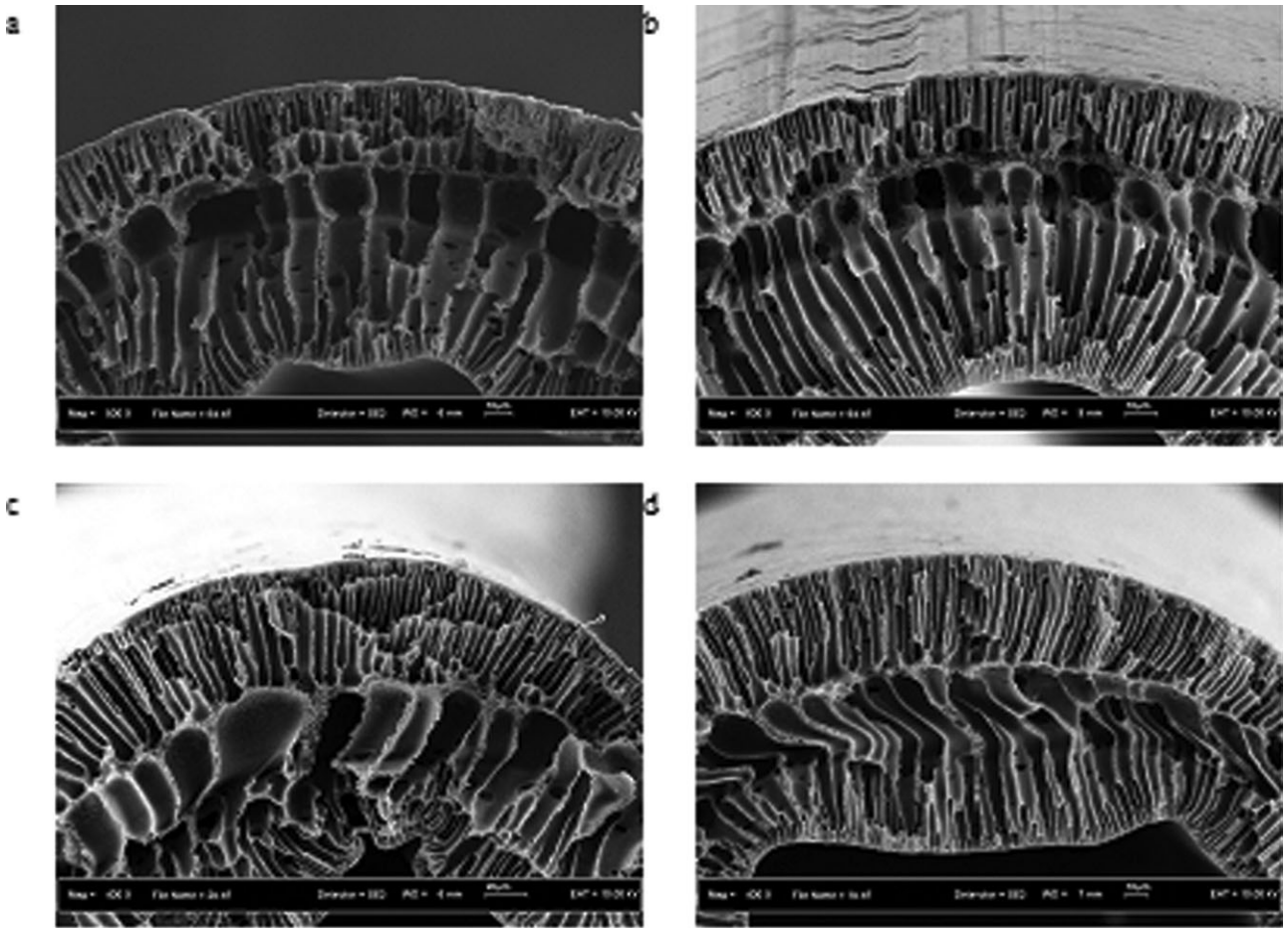

Figure 11. Cross-sectional SEM micrographs of membranes (a) M2, (b) M4, (c) M13, and (d) M14.

hollow-fiber membranes by a dry–wet spinning method. The performance of the fabricated membranes in contactor applications was investigated with pure CO_2 in the lumen side and distilled water in shell side of a contactor and compared with the performance of a commercial PVDF membrane supplied from Tianjin Motian Membrane Engineering Technology Co., Ltd. China. The results show that the membrane fabricated from 17 wt % PVDF, 3 wt % phosphorous acid, and 80 wt % NMP had the highest AR among the fabricated and commercial membranes; for example, the AR at V_{liquid} = 0.4 m/s was 1.2×10^{-3} mol m^{-2} s^{-1}.The AR of membrane M12 was 2.58×10^{-3} mol m^{-2} s^{-1} at the same V_{liquid}; this value was 115% higher than the AR mentioned previously.

Wang et al.[29] used a commercial membrane contactor, the Celgard MiniModule 0.75×5, and investigated the AR of CO_2 in the case of water in the lumen side as an absorbent and pure CO_2 in the shell side of a contactor. At V_{liquid} = 0.4 m/s, the AR of CO_2 for membrane M12 (2.58×10^{-3} mol m^{-2} s^{-1}) was 416% higher than the AR of the commercial contactor, which was 0.5×10^{-3} mol m^{-2} s^{-1}.

Atchariyawut et al.[30] investigated the performance of a commercial hydrophobic PVDF membrane from Memcor (South Windsor, New South Wales, Australia) in contactor applications. Both the physical and chemical absorption of CO_2 were studied. They used water and a 2*M* NaOH solution as absorbents on the lumen side of the contactor, and pure CO_2 flowed on the shell side. At V_{liquid} = 1 m/s, the CO_2 flux values were 1.1×10^{-3} and 3.5×10^{-3} mol m^{-2} s^{-1} for physical and chemical absorption, respectively. The AR of CO_2 for membrane M12 at V_{liquid} = 1 m/s was 3.49×10^{-3} mol m^{-2} s^{-1}; this was 217% higher than the AR of the commercial PVDF membrane in the case of physical absorption and nearly equal in the case of chemical absorption.

Dindore et al.[31] used commercial polypropylene hollow-fiber membranes (Accurel Q3/2, Membrana GmbH, Germany) and reported the AR of CO_2 in the membrane contactor as water flowed on the lumen side of contactor. The AR at V_{liquid} = 0.5 m/s was 2.53×10^{-3} mol m^{-2} s^{-1}; this was 9% lower than the AR of CO_2 for membrane M12 (2.77×10^{-3} mol m^{-2} s^{-1}).

The SEM micrographs for the cross sections of membranes M2, M4, M13, and M14 are shown in Figure 11. The structures of these membranes were almost the same as those of membranes M5, M6, and M16, as presented in our earlier article.[19] Fingerlike macrovoids originated from the inner and outer surfaces of the membranes and extended to the middle

section. The low viscosity and thermodynamic stability of the polymer solution and the application of strong internal and external coagulants (water) worked together to offer proper conditions for the penetration of the coagulant toward the center of the cross section, and this led to the formation of the fingerlike macrovoids.

CONCLUSIONS

SMMs were used to alter the hydrophobicity of PEI hollow-fiber membranes, and the effect of three fabrication parameters, PEI and SMM concentration in the spinning dope and air gap, on the properties of the membranes in terms of the LEPw and AR of CO_2 in the membrane gas absorption process were investigated with RSM. The conclusions are as follows:

1. Compared to PEI membranes without SMMs, the SMM-modified membranes generally had higher AR and lower LEPw values.
2. The regression model developed for the LEPw satisfied the criterion for regression, but it had a low goodness of fit; this could have been related to the test procedure. The model predicted that LEPw would decrease as the air gap increased. This was confirmed by SEM, which showed a pore size increase with increasing air gap. The model further predicted a minimum point for variation of the LEPw versus SMM weight percentage and an increase in the LEPw as PEI (wt %) increased.
3. The model developed for the AR of CO_2 satisfied the criteria for regression and lack of fit, had a high R^2 and adjusted R^2, and was accurate. The model predicted interactions between the fabrication parameters on response; this could have been related to the effects of different characteristics of the membrane on the AR.
4. The AR of CO_2 for the SMM-surface-modified membrane was compared with the AR of CO_2 for the hydrophobic membranes made in-house and commercially and showed the superior performance of the surface-modified membrane; this could have been related to their big pore size, high membrane porosity, and low membrane wettability and tortuosity.

REFERENCES

1. Yeon, S. H.; Lee, K. S.; Sea, B.; Park, Y. I.; Lee, K. H. *J. Membr. Sci.* **2005**, *257*, 156.
2. Khayet, M. *Adv. Colloid Interface Sci.* **2011**, *164*, 56.
3. Dindore, V. Y.; Brilman, D. W. F.; Geuzebroek, F. H.; Versteeg, G. *F. Sep. Purif. Technol.* **2004**, *40*, 133.
4. Bakeri, G.; Matsuura, T.; Ismail, A. F. *J. Membr. Sci.* **2011**, *383*, 159.
5. Yip, J.; Chan, K.; Sin, K. M.; Lau, K. *S. Appl. Surf. Sci.* **2006**, *253*, 2493.
6. Yan, M. G.; Liu, L. Q.; Tang, Z. Q.; Huang, L.; Li, W.; Zhou, J.; Gu, J. S.; Wei, X. W.; Yu, H. *Y. Chem. Eng. J.* **2008**, *145*, 218.
7. Belfer, S.; Fainshtain, R.; Purinson, Y.; Gilron, J.; Nyström, M.; Mänttäri, M. *J. Membr. Sci.* **2004**, *239*, 55.
8. Chennamsetty, R.; Escobar, I.; Xu, X. *J. Membr. Sci.* **2006**, *280*, 253.
9. Ulbricht, M.; Matuschewski, H.; Oechel, A.; Hicke, H. G. *J. Membr. Sci.* **1996**, *115*, 31.
10. Geuskens, G.; Etoc, A.; Di Michele, P. *Eur. Polym. J.* **2000**, *36*, 265.
11. Qiu, C.; Nguyena Liheng Zhang, Q. T.; Ping, Z. *Sep. Purif. Technol.* **2006**, *51*, 325.
12. Bolong, N.; Ismail, A. F.; Salim, M. R.; Rana, D.; Matsuura, T. *J. Membr. Sci.* **2009**, *331*, 40.
13. Khulbe, K. C.; Feng, C. Y.; Matsuura, T.; Mosqueada-Jimenaez, D. C.; Rafat, M.; Kingston, D.; Narbaitz, R. M.; Khayet, M. *J. Appl. Polym. Sci.* **2007**, *104*, 710.
14. Khayet, M.; Mengual, J. I.; Matsuura, T. *J. Membr. Sci.* **2005**, *252*, 101.
15. Pham, V. A.; Santerre, J. P.; Matsuura, T.; Narbaitz, R. M. *J. Appl. Polym. Sci.* **1999**, *73*, 1363.
16. Qtaishat, M.; Khayet, M.; Matsuura, T. *J. Membr. Sci.* **2009**, *329*, 193.
17. Suk, D. E.; Pleizier, G.; Deslandes, Y.; Matsuura, T. *Desalination* **2002**, *149*, 303.
18. Bakeri, G.; Matsuura, T.; Ismail, A. F.; Rana, D. *Sep. Purif. Technol.* **2012**, *89*, 160.
19. Bakeri, G.; Ismail, A. F.; Rana, D.; Matsuura, T.; Shariaty, M. *J. Appl. Polym. Sci.* **2012**, *123*, 2812.
20. Xiangli, F.; Wei, W.; Chen, Y.; Jin, W.; Xu, N. *J. Membr. Sci.* **2008**, *311*, 23.
21. Suk, D. E.; Matsuura, T.; Park, H. B.; Lee, Y. M. *J. Membr. Sci.* **2006**, *277*, 177.
22. Ismail, A. F.; Dunkin, I. R.; Gallivan, S. L.; Shilton, S. J. *Polymer* **1999**, *40*, 6499.
23. Ismail, A. F.; Kumari, S. N. *J. Membr. Sci.* **2004**, *236*, 183.
24. Myers, R. H.; Montgomery, D. C.Response Surface Methodology: Process and Product Optimization Using Designed Experiments; Wiley: New York, **2002**.
25. Khaisri, S.; deMontigny, D.; Tontiwachwuthikul, P.; Jiraratananon, R. *Sep. Purif. Technol.* **2009**, *65*, 290.
26. Rajabzadeh, S.; Teramoto, M.; Al-Marzouqi, M. H.; Kamio, E.; Ohmukai, Y.; Maruyama, T.; Matsuyama, H. *J. Membr. Sci.* **2010**, *346*, 86.
27. Mavroudi, M.; Kaldis, S. P.; Sakellaropoulos, G. P. *J. Membr. Sci.* **2006**, *272*, 103.
28. Atchariyawut, S.; Feng, C.; Wang, R.; Jiraratananon, R.; Liang, D. T. *J. Membr. Sci.* **2006**, *285*, 272.
29. Wang, R.; Zhang, H. Y.; Feron, P. H. M.; Liang, D. *T. Sep. Purif. Technol.* **2005**, *46*, 33.
30. Atchariyawut, S.; Jiraratananon, R.; Wang, R. *Sep. Purif. Technol.* **2008**, *63*, 15.
31. Dindore, V. Y.; Brilman, D. W. F.; Feron, P. H. M.; Versteeg, G. F. *J. Membr. Sci.* **2004**, *235*, 99.